

# An instrumented driven pile in Dublin boulder clay

*E. Farrell, BA, BAI, MS, PhD, FIEI, MICE, FGS, B. Lehane, BE, DIC, PhD, MIEI and M. Looby, BA, BAI, MSc*

■ Precast concrete piles, driven to a set in Dublin black boulder clay, have been used extensively in Dublin where depths of fill or soft soil make shallow foundations uneconomical. This paper describes the results of a test pile which was instrumented with vibrating wire gauges and pore pressure probes at various levels along the pile shaft. Three compression tests were carried out on the test pile: one within 2.4 h of its installation, one after 1.8 days and one after 17 days. Finally, a tension (pull-out) test was carried out after 24 days. The loading tests showed that there was a significant increase in both the ultimate shaft and base capacity with time and that about 60% of the total pile capacity was achieved in end-bearing in all three compression tests. The last compression test on the pile, which was carried out when all of the excess pore pressure set up by driving had dissipated, indicated an apparent  $N_c$  value of over 50 when applied to the in situ undrained shear strength of the boulder clay prior to the test. An analysis of the base displacement and pore pressures during load indicated that this high  $N_c$  value is likely to be due to an increase in the mean effective stress at the pile tip due to its insertion.

**Keywords:** piles & piling; geotechnical engineering

## Notation

|           |  |
|-----------|--|
| $c_h$     | horizontal coefficient of consolidation  |
| $c_u$     | undrained shear strength   |
| $D$       | pile diameter  |
| $G$       | shear modulus  |
| $h$       | distance from the base of the pile   |
| $N$       | standard penetration test $N$ value  |
| $N_c$     | bearing capacity factor on cohesion  |
| OCR       | overconsolidation ratio  |
| $P$       | total pile head load   |
| $p'$      | mean effective stress  |
| $q_b$     | pile end-bearing stress  |
| $q_{ult}$ | ultimate base bearing capacity   |
| $R$       | pile radius  |
| $T_{su}$  | time interval between driving and testing the pile   |
| $\alpha$  | adhesion factor = ratio of the average shear stress mobilized on the shaft to the undrained shear strength of the soil |

|              |  |
|--------------|--|
| $\delta$     | interface friction angle                                     |
| $\delta_b$   | pile base displacement                                       |
| $\delta_H$   | pile head displacement                                       |
| $\epsilon_s$ | triaxial shear strain  |
| $\tau_f$     | ultimate local shaft shear stress                            |
| $\phi'_{cv}$ | critical state effective stress angle of shearing resistance |

## Introduction

Driven precast concrete piles have been used extensively in Dublin on sites where the depths of fill or soft soil make traditional foundations uneconomical. These are normally driven to a set in the boulder clay which underlies most of the city. Although the performance of these piles has generally been satisfactory, problems were experienced on one large development, the Tallaght town centre,<sup>1</sup> which highlighted a lack of detailed understanding of the behaviour of piles driven into boulder clay.

2. This paper describes the results of field experiments with an instrumented tubular steel pile which was driven into Dublin boulder clay.<sup>2</sup> The aim of these experiments, which were undertaken as part of a research project at Trinity College Dublin (TCD), was to improve the understanding of the factors governing the axial load capacity of driven piles in hard glacial tills. The results, although comparing well with trends shown in other instrumented pile test programmes, challenge some of the commonly held assumptions made in standard design practice.

## Instrumented pile test

### Pile description

3. The TCD pile was a 273 mm diameter, 7.5 m long, steel closed-end tubular pile. The pile wall thickness was 10 mm and the base was formed from a flat 20 mm thick, 273 mm diameter steel disc. The lower 3.5 m of the pile were instrumented with vibrating wire strain gauges and pore pressure probes. The axial stiffness of this steel pile was similar to that of a 250 mm square precast concrete pile and also had approximately the same base area (0.0745 m<sup>2</sup> for the steel pile compared with 0.0625 m<sup>2</sup> for a 250 mm square concrete pile).

### Pile instrumentation

4. The pile configuration is shown in Fig. 1 which also lists the height of each instrument above the pile base ( $h$ ) normalized by the pile

*Proc. Instn  
Civ. Engrs  
Geotech. Engng,  
1998, 131, Oct.,  
233-241*

*Paper 11564*

*Written discussion  
closes 15 February 1999*

*Manuscript received  
15 October 1996;  
revised manuscript  
accepted 23 April 1998*



*Eric Farrell,  
Senior Lecturer,  
Trinity College,  
Dublin*



*Barry Lehane,  
Lecturer,  
Trinity College,  
Dublin*



*Michael Looby,  
Senior Project  
Engineer, Ove Arup  
& Partners,  
Ireland*

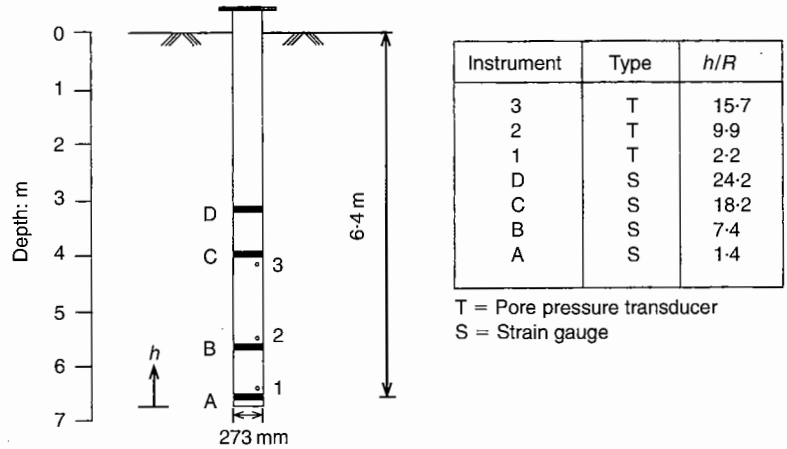
radius ( $R$ ). The lower 3.5 m of the pile were cut into three sections to facilitate fixing and calibration of the instrumentation. These sections were subsequently welded together with the outer surface of the weld made flush with that of the pile. The cables of the instrumentation passed up the centre of the pile and through a pre-drilled hole near the pile head for connection to a portable measuring unit.

5. Twelve 150 mm long vibrating wire gauges, three at four different levels, were welded to the inside surface of the pile; the three gauges at each level were spaced equally around the circumference. All gauges were encapsulated in resin to minimize the risk of damage due to the shock waves imposed during driving. The gauges were calibrated in the laboratory by loading the individual instrumented sections prior to their reassembly. The percentage difference between the manufacturer's quoted gauge factor and those measured was typically less than 3%.

6. Pore pressure probes, as shown on Fig. 1, which were positioned at three levels over the lower 2.5 m of the pile, comprised pressure transducers housed in specially milled 50 mm diameter plastic mounting blocks at the centre of which 13 mm diameter sintered steel porous discs were positioned. Immediately prior to the start of pile driving, the gap between the porous stone and the face of the transducer was filled with de-aired silicone oil and the stones (also saturated in silicone oil) were inserted into the mounting block. The pore pressure probe design was based on that reported by Bond *et al.*<sup>3</sup>

*Ground conditions*

7. The ground conditions in the Dublin area generally comprise brown boulder clay overlying



black boulder clay which in turn is underlain by limestone bedrock (Fig. 2). Both boulder clays belong to the same lodgement till deposit, the former being the weathered surface of the latter. These deposits are often overlain by made ground and by estuarine or alluvial deposits within the flood plain of the River Liffey.

8. The general properties of the brown and black boulder clay have been presented by Farrell *et al.*<sup>4</sup> Both contain a well-graded mixture of particle sizes ranging from clays to cobbles and have a fines content (<0.063 mm) of about 35%. The coefficient of permeability of the black boulder clay<sup>5</sup> is  $\sim 10^{-9}$ – $10^{-10}$  m/s. Layers or lenses of sand, gravel or glacio-lacustrine deposits can occasionally occur within the mass of the soil. The black boulder clay is generally very stiff or hard and its strength, together with its stone content, make it difficult to sample.

9. The TCD pile test programme was carried out at the site of a major development of

Fig. 1. Instrumentation configuration

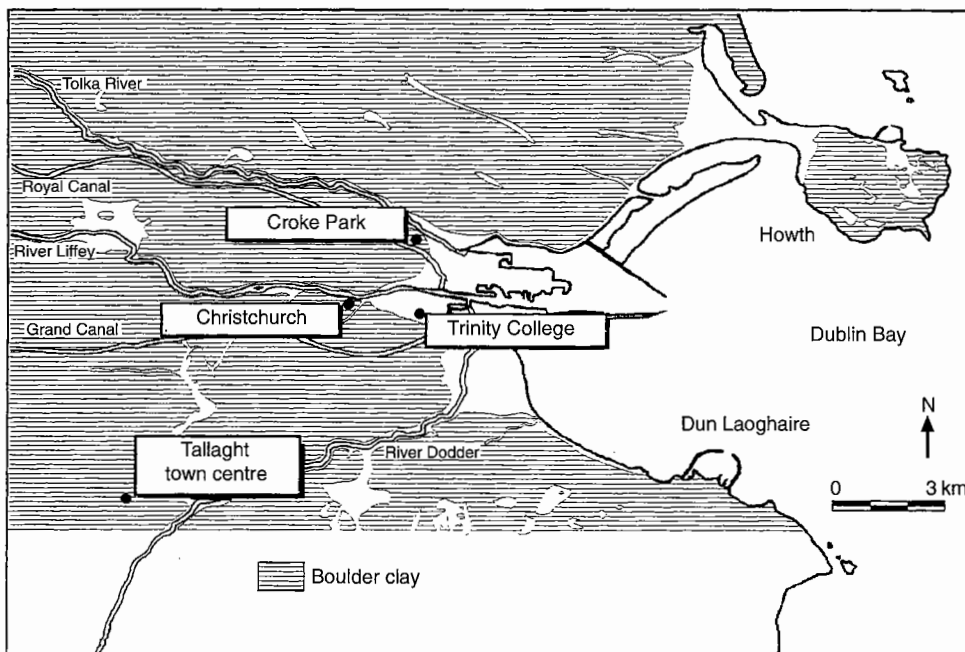


Fig. 2. Extent of boulder clay in the Dublin area

The Gaelic Athletic Association's stadium at Croke Park in Dublin (Fig. 2). A cable percussive borehole put down adjacent to the test pile location (Fig. 3) encountered 2 m of made ground over 1.65 m of stiff brown sandy gravelly clay with some clayey gravel (brown boulder clay) over very stiff/hard black sandy gravelly clay (black boulder clay). Boreholes for the stadium development indicated that the black boulder clay extended to a depth of about 15 m and was underlain by a dense angular gravel stratum which extended to the limestone bedrock at about 20 m depth. Groundwater level was at about 2.5 m depth.

10. Standard penetration tests (SPTs) carried out in the borehole adjacent to the pile test location recorded an  $N$  value of 33 for the brown boulder clay and  $N$  values of between 65 and 80 for the black boulder clay, with many refusals. The  $N$  values recorded in all boreholes at the site are plotted on Fig. 3; these indicate no systematic variation in  $N$  with depth. The moisture contents (determined on the entire sample) and liquid and plastic limits, shown in Fig. 4, are consistent with values expected for a heavily overconsolidated low plasticity till.

11. The vertical yield stress measured in a standard (24 h) incrementally loaded oedometer test on a sample from 5 m depth (which was loaded to a maximum stress of 10 MPa) was 1200 kPa. This indicates that the overconsolidation ratio (OCR) of the black boulder clay over the lower 3 m of the pile shaft length is in the range 12–20.

12. The triaxial compression undrained shear strength of the black boulder clay interpreted from field and laboratory tests is about 450 kPa. Undrained and drained triaxial tests indicate a strong tendency for the material to

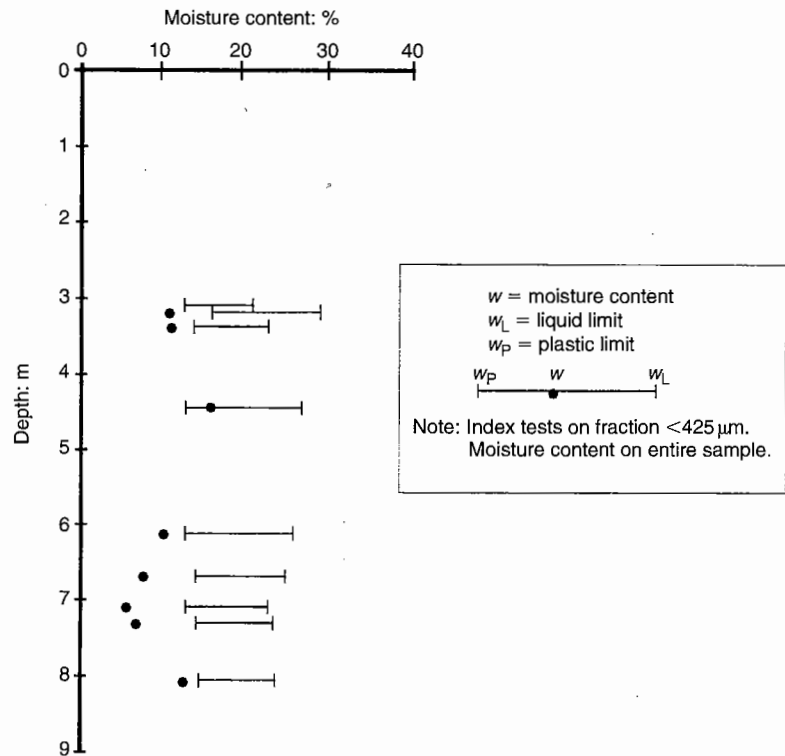
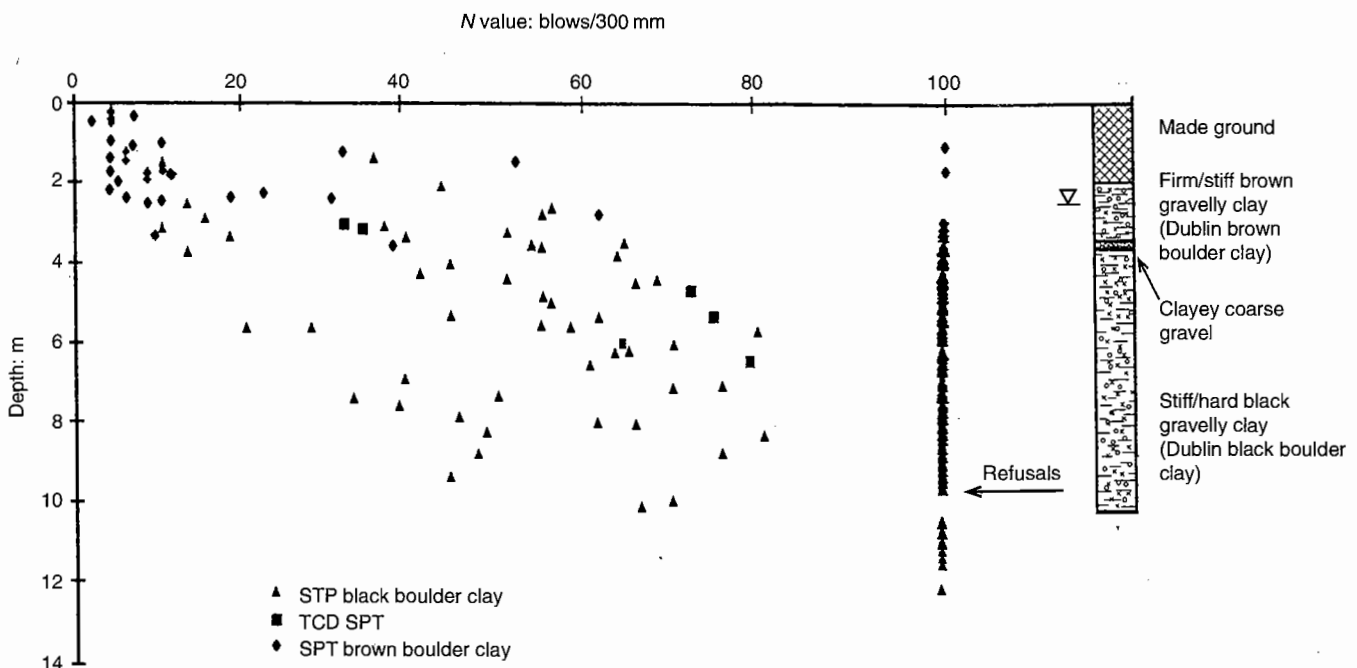


Fig. 4. Moisture content, liquid and plastic limits

dilate as it approaches a critical state at  $\phi'_{cv} = 37^\circ$ . This high  $\phi'_{cv}$  is consistent with that to be expected from the black boulder clay considering the high 'rock flour' component of its clay fraction. Typical shear moduli normalized by mean effective stress ( $G/p'$ ) measured in triaxial compression tests after anisotropic consolidation and swelling, typically reduce from  $1000 \pm 300$  at a triaxial shear strain ( $\epsilon_s$ ) of 0.01% to  $250 \pm 70$  at  $\epsilon_s = 0.1\%$ .

13. Laboratory shear box interface tests

Fig. 3. Standard penetration test results and borehole log



suggested that the interface friction angle ( $\delta$ ) between the black boulder clay and the outside of the steel pile is about  $32^\circ$ .

**Instrumented pile test programme**

14. The pile was driven using a Banut 4 t hammer (fall height of 300 mm) to a depth of 6 m, and after 1 h was redriven to a final depth of 6.4 m with a set of 12 drops/25 mm. This relatively low set (compared with the set of 20–25 drops per 25 mm used in practice with this hammer on a 300 mm square precast concrete pile) was selected so that it would be possible, with the available kentledge of 1400 kN, to reach the ultimate shaft capacity of the pile during subsequent load tests.

15. The pile testing programme included three compression tests carried out at different time intervals after driving, followed by one tension (pull-out) test. The testing programme is summarized in Table 1 which also lists the time interval between driving and testing ( $T_{su}$ ). The pile head load against displacement plot for the compression tests are shown in Fig. 5. It was necessary to unload the pile during test 3 at 930 kN before applying the maximum load of 1350 kN to improve the alignment of the jack; this reload loop, which followed the original load displacement curve, has been omitted for clarity.

16. The pile loading rate that was chosen was expected to provide undrained loading conditions. The load increments/decrements varied from 100 to 150 kN and were maintained for 5 min.

**Load and displacement behaviour**

17. The maximum axial pile head loads applied and details concerning the overall shaft and base loads are included in Table 1. The loads at different elevations of the test pile have been assessed from the strain gauge readings related to the unstrained pile prior to its installation. The loads therefore include all residual loads induced by the driving and test procedure. There was no noticeable drift in the vibrating wire gauges used and this lack of drift was confirmed by the zero strain readings recorded near the pile base at the ultimate load in the tension test.

18. It is immediately evident from the results presented in Table 1 that there is a

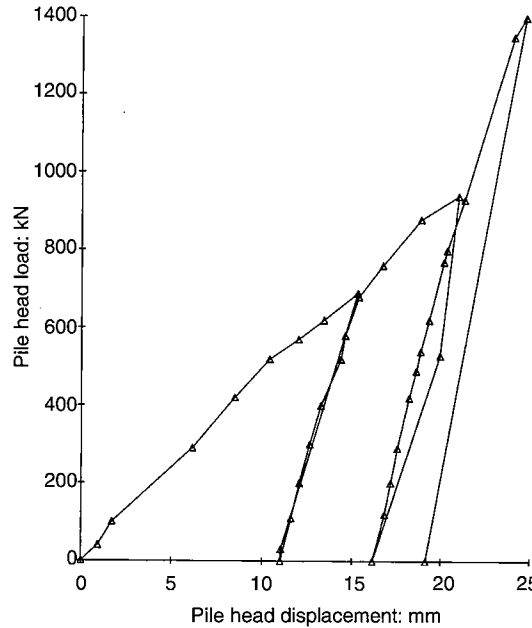


Fig. 5. Load plotted against cumulative pile head displacement

considerable increase in both the base and shaft loads as  $T_{su}$  increases. The increase in the pile capacity with  $T_{su}$  is also evident from the load/settlement results which are given in Fig. 6. It is apparent that the tension (pull-out) shaft capacity is only 80% of the compressive shaft capacity (measured in test 3C) and the former required a larger pile head displacement for full mobilization.

19. The increase in the shear stress on the shaft (averaged over the lower 3.5 m length of the pile) with pile head displacement ( $\delta_H$ ) in the three compressive load tests is shown in Fig. 7. All curves show a ductile response. Ultimate average shear stresses were developed in all tests except in test 3C where the shear stresses are estimated to have reached  $\approx 80\%$  of ultimate values.

20. The variation in the pile end-bearing stress ( $q_b$ ) with the displacement at the pile base ( $\delta_b$ ) is shown in Fig. 8 for the three compression load tests. The ultimate base bearing capacity ( $q_{ult}$ ) was estimated using a hyperbolic extrapolation to 10% of the pile diameter in those tests which did not reach this condition. Only data recorded past the reload portions of the curves were used for this extrapolation. The  $q_{ult}$  value of 25 MPa assessed

Table 1. Summary of test results

| Test No. | Test type | $T_{su}$ days | Max. applied load: kN | $\delta_H$ at max. load: mm | Max. shaft load: kN | Base load: kN | Base load as % of max. applied load | $\alpha$ -value ( $c_u = 450$ kPa) |
|----------|-----------|---------------|-----------------------|-----------------------------|---------------------|---------------|-------------------------------------|------------------------------------|
| 1C       | Comp.     | 0.1           | 720                   | 15                          | 279                 | 441           | 61                                  | 0.21                               |
| 2C       | Comp.     | 1.8           | 944                   | 10                          | 336                 | 608           | 64                                  | 0.25                               |
| 3C       | Comp.     | 17            | 1350(2200*)           | 7.5                         | 546(750*)           | 1450*         | 66*                                 | 0.55*                              |
| 4T       | Tension   | 24            | -450                  | -14                         | -450                | —             | —                                   | 0.4                                |

\* Extrapolated to ultimate conditions (see Figs 6 and 7).

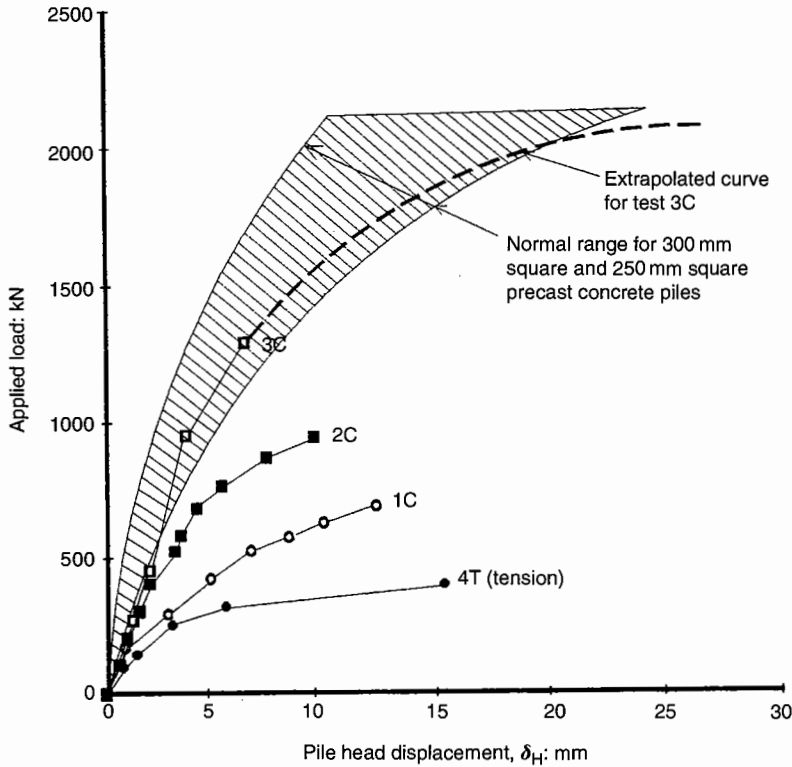


Fig. 6. Comparison of test pile load/displacement curves with load/displacement range measured in practice

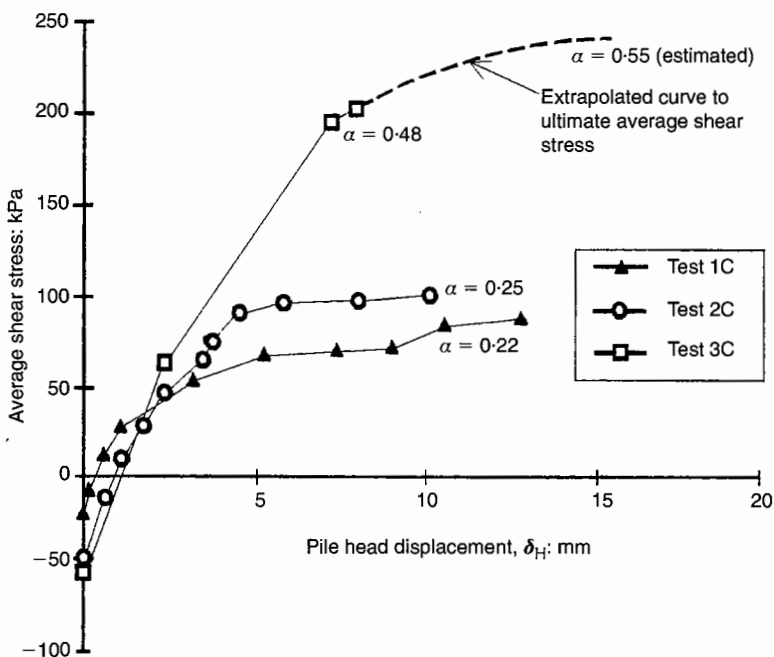


Fig. 7. Average shear stress on shaft in compression tests

for the last compressive load test (commenced after full equalization of pore pressure) was less than but compatible with that interpreted from static load tests on 250 mm square concrete piles driven to similar depths in the black boulder clay (Fig. 6).

#### Pore pressures response

21. The pore pressures measured at the pile-soil interface during driving were low and frequently negative (i.e. below atmospheric pressure). Once driving had ceased, pressures

increased rapidly and reached values of up to 750 kPa. The dissipation of these pressures over time is shown in Fig. 9 which indicates that hydrostatic conditions had effectively been re-established after about a week. Tests 3C and 4T were performed after full dissipation of excess pore pressures.

22. The pore pressures measured during load testing reduced significantly as loading continued in the first test (1C) but remained virtually constant (showing very slight increases) in tests 2C and 3C. No pore pressure

measurements were obtained in the tension test (4T) due to an instrumentation fault.

**Load distribution on pile during tests**

23. The load distribution along the pile during the initial test (test 1C) is shown in Fig. 10. Although this test was carried out just 2 h after driving (when the excess pore pressures were very high), the loading distribution shows features common to all compression tests

- (a) the presence of a residual base load (increasing from  $\approx 50$  kN prior to test 1C to  $\approx 140$  kN prior to test 3C)
- (b) over 60% of the ultimate pile load being taken by the base
- (c) the rate of load transfer from the shaft to the ground increasing with depth and being negligible over the upper 3-7 m of the pile.

The pile capacity is therefore almost entirely derived from the resistance provided by the black boulder clay.

24. The distribution of the shaft shear stress at maximum loading (as interpreted from the gradients of load distributions) determined in all tests is shown in Fig. 11. Shear stresses are seen to increase with depth below 3.5 m in the compression test while, in the tension test, it is evident that little resistance is provided by the clay down to  $\approx 5$  m depth and that  $\approx 75\%$  of the capacity is supplied by the bottom metre of the pile shaft. There was no noticeable variation in the loads or pore pressures over the period of application of each load increment.

25. The base load was approximately zero at the ultimate tension load, confirming the reliability of the initial zero readings adopted for the vibrating wire gauges.

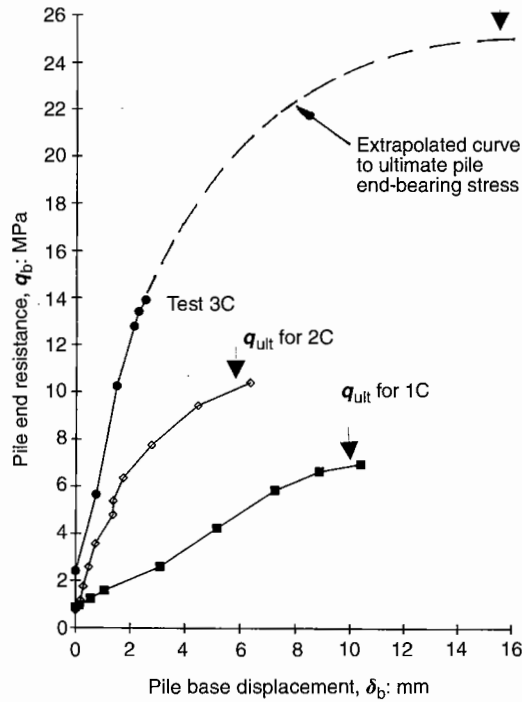


Fig. 8. Pile end-bearing stress

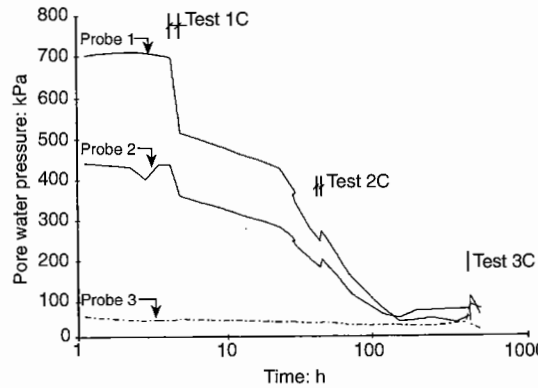


Fig. 9. Pore water pressure at pile-soil interface

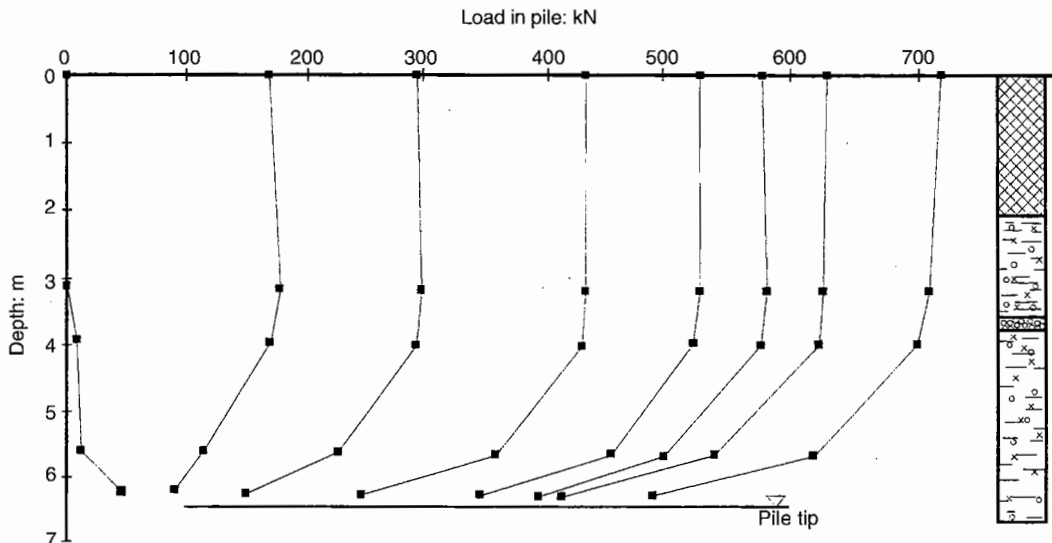


Fig. 10. Load distribution on pile during test 1C

## Discussion on behaviour of test pile

### Pore pressure

26. The low or sub-atmospheric pore water pressures recorded during pile driving are typical of the response measured at the pile-soil interface of heavily overconsolidated clays which tend to dilate when sheared. The rapid increase in the pore water pressure once driving ceased is consistent with the inflow of water from a zone of high pore pressure generated within the soil outside the immediate pile-soil interface shear zone.<sup>6</sup>

27. The subsequent dissipation of excess pore water pressure to hydrostatic conditions, assuming linear consolidation and the time factors proposed by Houlsby and Teh<sup>7</sup> with a rigidity index of 150, is compatible with horizontal coefficients of consolidation ( $c_h$ ) of  $\approx 35 \text{ m}^2/\text{year}$  at  $h/R = 2$  ( $z = 6.1 \text{ m}$ ) and  $\approx 100 \text{ m}^2/\text{year}$  at  $h/R = 10$  ( $z = 5 \text{ m}$ ), where  $h$  is the distance from the base of the pile,  $R$  is the pile radius and  $z$  is the depth below ground level. These coefficients are within the bounds normally encountered adjacent to driven piles in low plasticity clays.<sup>8</sup>

28. Pore pressures reduced during test 1C but remained constant or increased in subsequent load tests. This tendency for dilation during shear at the early stages of equalization is a characteristic of both lightly and heavily overconsolidated clays and is indicative of the high degree of pseudo-overconsolidation of the clay at this stage.<sup>8</sup> Shaft capacities do not, for this reason, show a direct correlation with the pre-loading pore pressures (or more precisely with the pre-loading radial effective stresses).

### Shaft capacity

29. The  $\alpha$  method for estimating the shaft shear stress under ultimate loading conditions has traditionally been used in the calculation of pile capacities in boulder clay, the average shaft shear stress (skin friction) being assumed equal to  $\alpha c_u$ . The average shaft shear stress (i.e. the mean stress over the length of the pile in the boulder clay) is shown in Fig. 7. Taking  $c_u = 450 \text{ kPa}$ ,  $\alpha$  is 0.22 for test 1C when the excess pore water pressure was high. The shaft capacity rose subsequently and, in the final compression test (when the excess pressures had dissipated),  $\alpha$  is estimated to reach about 0.55 if the pile had been taken to failure. This latter coefficient is comparable to the value of 0.45 normally used in Dublin design practice.

30. The local shaft shear stress ( $\tau_f$ ) distribution along the pile was non-linear with the maximum shaft shear stress occurring at the pile tip (Fig. 11). This distribution clearly contrasts with that which would be implied by the  $\alpha$  method (i.e. a uniform  $\tau_f$  value for a deposit with a relatively constant  $c_u$  value). This is compatible with that predicted by the new

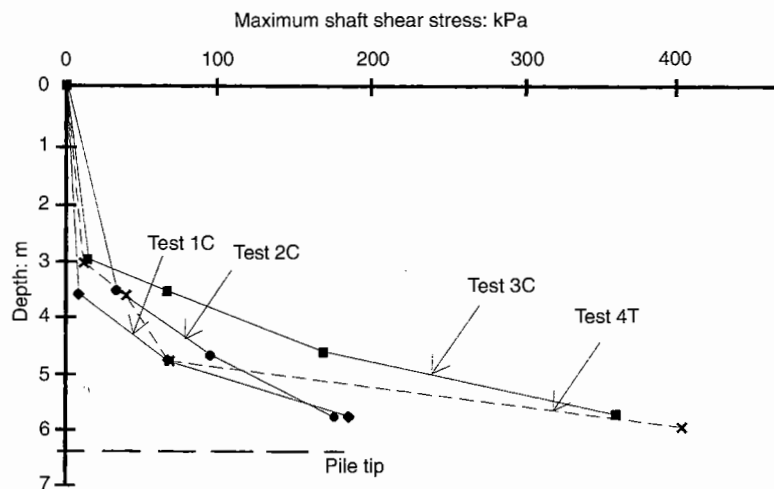


Fig. 11. Shaft shear stress at maximum loading

Imperial College method<sup>9</sup> which suggests that in any given soil horizon  $\tau_f$  will reduce with the distance from the base of the pile.

31. The ultimate shaft capacity of the Croke Park test pile in the tension test was about 80% of its compressive shaft capacity. This ratio of tension to compressive shaft capacity is similar to that measured in the lodgement till at Cowden by Lehane and Jardine<sup>10</sup> who showed that the apparent interface friction angle ( $\delta$ ) was significantly greater in compression than in tension. Such a phenomenon can be partly explained given that the dominant boundary conditions applying during compression and tension pile loading differ and by the likelihood that failure occurs within the soil at a short distance from the shaft.

### Base capacity

32. The ultimate base resistance increased from about 7.5 MPa in the initial test carried out 2h after driving, to an estimated ultimate value of about 25 MPa in the last test which was carried out following almost full dissipation of the excess pore water pressures. These base resistances were achieved on a pile which was driven to less demanding set than would normally be accepted in practice.

33. Using the simplistic assumption that the base of the pile can be modelled as a rigid plate on a linear elastic material, the  $q_b$  against  $\delta_b$  data in Fig. 8 imply an equivalent linear elastic shear modulus ( $G$ ) for the boulder clay at  $\delta_b/D = 1\%$  (or  $\delta_b = 2.7 \text{ mm}$ ) of 30 MPa, 140 MPa and 250 MPa in tests 1C, 2C and 3C respectively. All of these (reload) moduli are compatible with a  $G/p'$  value of 300 when  $p'$  (the mean effective stress) is derived by subtracting the excess pore pressures measured at  $h/R = 2$  at the start of each test from a final average mean effective stress of 750 kPa. The pile end-bearing stress at this level of loading may therefore be surmised to correlate directly with the measured pore pressure and to be proportional to the mean effective stress.

34. At higher values of  $\delta_b/D$ , dilation effects are likely to become significant, particularly at the early stages of equalization. For example, the slightly concave upwards portion of curve on Fig. 8 measured in test 1C suggests that dilation made a significant contribution to the ultimate end-bearing capacity in this test; ultimate shaft shear stresses in this test also benefited from large reductions in pore pressure.

35. The observation in ¶33 implies that the process of driving followed by equalization increased the mean effective stress in the vicinity of the pile base from an estimated initial value of  $\approx 150$  kPa to a final value of  $\approx 750$  kPa. Such an increase is compatible with the very high  $N_c$  value of 55 backfigured from the ultimate undrained end-bearing resistance in test 3C (25 MPa) using the till's initial *in situ* undrained shear strength ( $\approx 450$  kPa).

### Standard practice for driven precast concrete piles in Dublin

36. Square sectioned driven precast concrete piles, with side lengths varying from 250 to 350 mm, are the most popular driven piles in Dublin. The piles are usually driven to a penetration into the black boulder clay of between 2 and 4 m and are deemed acceptable when a required set is achieved. Contractors quote working loads within the range of about 700 and 1000 kN for the 250 and 350 mm square piles respectively.

37. The range of load displacement ( $P$  vs  $\delta_H$ ) curves obtained using standard practice on 250 and 300 mm square piles<sup>11</sup> are compared on Fig. 6 with the  $P$  vs  $\delta_H$  curves measured in the three compression load tests on the Croke Park test pile (the axial stiffness of the test pile approximated to that of a 250 mm square precast concrete pile). The test pile shows a progressive increase in ultimate capacity and stiffness from test 1C to test 3C, with the latter's  $P$  vs  $\delta_H$  characteristics being within the (but to the lower bound) of standard range (despite the lower than normal set to which the pile was driven).

38. The load distribution predicted from the results of a CAPWAP dynamic pile test on a 250 mm square precast concrete pile (driven to a standard set) is shown in Fig. 12 and is seen to be very similar to that in test 3C. Moreover, the interpreted base capacity is in good agreement with that indicated by the instrumented pile test. This comparison serves to confirm the usefulness of carefully performed and interpreted dynamic pile tests.

### Conclusions

39. The pore water pressure response around the TCD instrumented pile (closed-end 273 mm steel tubular pile) was broadly similar to that recorded by others on instrumented piles driven into heavily overconsolidated glacial

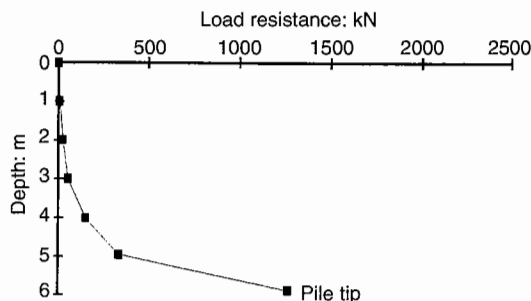


Fig. 12. Resistance distribution predicted by CAPWAP dynamic test at Tallaght

clays. The till exhibited a strong tendency for dilation (or reduction in pore pressures) when sheared in a partially equalized condition.

40. Both the ultimate shaft and end-bearing capacity increased significantly with time.

41. The distribution of shaft shear stress during compression and tension loading was non-linear, the greatest resistance being at the toe of the pile. The tests confirmed the inadequacy of the  $\alpha$  method for predicting shaft resistance.

42. The ultimate shaft resistance in tension testing was only 80% of that recorded in compression with about 75% of this capacity being from the bottom metre of the pile shaft.

43. About 60% of the ultimate capacity of the TCD test pile was achieved in end-bearing. Such a high percentage is more consistent with the ratio normally expected from a pile in a free-draining sand or gravel, despite the fact that the pile end-bearing was essentially undrained.

44. The ultimate undrained end-bearing resistance of a pile in Dublin boulder clay benefits considerably from the process of pile driving.

### Acknowledgements

45. This project was funded by Murphy International (Ireland) Ltd and by the Irish American Partnership. Irish Geotechnical Services Ltd kindly put down the borehole adjacent to the test pile.

### References

1. ARMISHAW J. W. and BUNNI N. G. Driven precast concrete piles in Dublin black boulder clay. In *Piling in Europe*. Thomas Telford, London, 1992, 219–226.
2. LOOBY M. *Investigation of the Behaviour of Driven Piles in Overconsolidated Clay*. MSc thesis, University of Dublin, Trinity College, 1996.
3. BOND A. J., JARDINE R. J. and DALTON J. C. P. The design and performance of the Imperial College instrumented pile. *American Society for Testing Materials, Geotechnical Testing Journal*, 1991, **14**, 413–424.
4. FARRELL E. R., COXON P., DOFF D. H. and PRIEDHOMME L. The genesis of brown boulder clay of Dublin. *Quarterly Journal of Engineering Geology*, 1995, **28**, 143–152.
5. FARRELL E. R., BUNNI N. G. and MULLIGAN J. The bearing capacity of Dublin black boulder clay.

- Transactions of the Institution of Engineers of Ireland*, 1988/89, **112**, 77-104.
6. BOND A. J. and JARDINE R. J. Effects of installing displacement piles in a high OCR clay. *Géotechnique*, 1991, **41**, 341-363.
  7. HOULSBY G. T. and TEH C. I. Analysis of the piezocone in clay. *Proceedings of the 1st International Symposium on Penetration Testing*, 1988, **2**, 777-783.
  8. LEHANE B. M. *Experimental Investigations of Pile Behaviour Using Instrumented Field Piles*. PhD thesis, University of London (Imperial College), 1992.
  9. JARDINE R. J. and CHOW F. C. *New Design Methods for Offshore Piles*. MTD publication 96/103, 1996.
  10. LEHANE B. M. and JARDINE R. J. Displacement pile behaviour in glacial clay. *Canadian Geotechnical Journal*, 1994, **31**, 79-90.
  11. FARRELL E. R., LEHANE B. M. O'BRIEN S. and ORR T. Stiffness of Dublin black boulder clay. *Proceedings of the XI European Conference*, Copenhagen, 1995, **1**, 109-114.
  12. LOOBY M., FARRELL E. R. and LEHANE B. M. Driven piles in boulder clay - design and practice. *Transactions of the Institution of Engineers of Ireland*, 1995/96, **119**, 89-106.